Chemical and Process Engineering Research
ISSN 2224-7467 (Paper) ISSN 2225-0913 (Online)
Vol.43, 2016

Adsorptive Removal of Erythrosin B Dye onto *Terminalia Catappa* Endocarp Prepared Activated Carbon: Kinetics, Isotherm and Thermodynamics Studies

Okoye, C. C[1*] Onukwuli, O. D[1] Okey-Onyesolu, C. F[1] Nwokedi, I. C[1]

1. Department of Chemical Engineering, Nnamdi Azikiwe University, PMB 5025, Awka, Anambra State, Nigeria

*****E-mail of the corresponding author: okoyecc7@gmail.com, cc.okoye@unizik.edu.ng

Abstract

The effectiveness of activated carbon prepared from Terminalia catappa (almond) endocarp via thermal and chemical activation for the adsorption of Erythrosin B (EB) dye was investigated. The thermally activated sample was impregnated with 60% by weight phosphoric acid (H_3PO_4) in 1:2 weight basis of activating agent to Terminalia catappa (almond) endocarp. Physico-chemical analyses results revealed the potential suitability of the prepared acid activated almond endocarp (AAAE) as an adsorbent. Further results obtained show that particle size, adsorbent dosage, pH, time, ion concentration and temperature had significant effect on the percentage of EB dye adsorbed. Freundlich model best fitted the experimental data compared to the results obtained for Langmuir and Dubnin-Radushkevich isotherm models. The adsorption kinetic data was modelled using the pseudo first-order, pseudo second-order and Elovich kinetic models. The kinetics of the adsorption process best followed the Elovich model. Thermodynamic parameters: Gibb's free energy (ΔG°), enthalpy change (ΔH°) and entropy change (ΔS°) were determined to evaluate the feasibility of the process and the effect of temperature on the system. The negative free energy obtained confirms the feasibility of the adsorption process. The adsorption of EB on the acid activated almond endocarp was found to be exothermic.

Keywords: Adsorption; Almond endocarp; Erythrosin B; Isotherm; Kinetics; Adsorption thermodynamics

1.0 Introduction

Dyes are major contributors to aquatic pollution. Textile, coke, paint, paper, pharmaceutical, etc industries generate effluents that have dyes as its constituent[1]. Effluents released from these dye-houses can be one of the biggest contributors to aquatic pollution[2,3]. In addition to aquatic pollution, dye effluents can negatively affect plant life thus detrimental to the entire eco system. Some dyes are also toxic and even carcinogenic[2]. Basic and reactive dyes are the most studied dye types in the dye contained effluent treatment. It is needful to remove/treat both of them[3]. Dyes are however non-degradable in nature, also stable toward light and oxidizing agents. These features pose challenge in the choice of the treatment method for dye contaminated wastewater[4].

Fenton-biological treatment scheme, photocatalytic and electrochemical combined treatment, adsorption, etc have been used in the treatment of dye contaminated wastewater[5]. In comparison to the removal methods of colours, it has been well established that adsorption is the most effective technique to remove colour from wastewater[4]. Thus, adsorption is widely employed as a purification method in many industrial processes[6].

Adsorption is one of the developed cost effective and efficacious methods of treating polluted water[7]. Activated carbon is the most frequently used adsorbent in purification, possessing a high adsorption potential due to its

physical and chemical structure[6]. High financial implication and rigourous procedure for the regeneration of conventional activated carbon deter its wide application. Therefore, it is of immense importance to develop cost effective and effective substitutes[7]. Consequently, several natural adsorbents have been used such as mesoporous egg shell membrane[8], peanut shell[9], Rice husk[10], jackfruit peel[5], palm shell powder[11], coffee husks[12].

In this study, the effectiveness of the locally sourced agricultural solid waste, almond endocarp (*Terminalia* catappa), to serve as a suitable adsorbent for the removal of EB dye was investigated. The ability of EB dye to be adsorbed onto solid materials informed its choice for this study. To achieve this aim, *Teminalia catappa* endocarp was thermally and chemically activated, characterized then batch adsorption experiments were evaluated. Conventional theoretical methods were employed to model the kinetics and equilibrium of the adsorption process. The thermodynamic study was made to generate thermodynamic parameters which describe the response of the system to temperature variation and also to examine the feasibility of the adsorption process.

2.0 Materials and methods

2.1 Adsorbate

The molecular formula, weight and maximum wavelength for the adsorbate (EB) are $C_{20}H_6I_4Na_2O_5$, 879.86gmol^{-1} and 528nm respectively. The structural formula for EB dye is shown in fig 1. A stock solution of 1000mg/L was prepared for EB dye by dissolving an appropriate quantity of EB dye in one litre of distilled water. The working solutions of desired concentrations were prepared by proper dilution of the stock solutions. Dilute solutions of HCl and NaOH were used to adjust the pH of the working solutions to desired values.

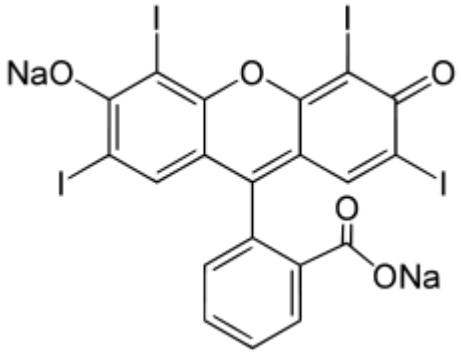

Fig 1: Structural formula for Erythrosin B

2.2 Adsorbent

2.2.1 Adsorbent development

The agro waste, almond endocarp (*Terminalia catappa*), was sourced from Nibo-Nise in Anambra state, Nigeria. The biosorbent was properly washed with distilled water and air dried. This assured the removal of contaminants such as sand, dirt, etc. The washed material was oven dried at temperature of 110^{o}C for 5 hours. The almond endocarp was reduced further to smaller particle sizes. Carbonization of the endocarp was carried out at Nigerian metallurgical institute, Onitsha, using a muffle furnace set at a temperature of 600 ℃ for one and half hours then was allowed to cool in a desiccator. The carbonized adsorbent was acid (H_3PO_4, 60% by weight) activated. Impregnation ratio of 1:2 weight basis of activating agent to adsorbent was employed. The slurry was vigorously stirred and allowed for 24 hours. The resulting carbon was rinsed with distilled water until the pH of the leachate was between

6-8 then dried in an oven at temperature of 105^0C for 5-6 hours. The oven dried activated carbon was reduced in size and sieved using mesh sizes between 75 µm – 850 µm.The activated carbon produced was stored in properly labelled air tight containers for further analyses and experiments. All chemicals for this research were all of analytical grade.

2.2.2 Adsorbent characterization

Physico-chemical characterization of the samples was done. The properties measured are percentage ash content, tapped bulk density, moisture content[13], pH (ASTMD 3838 – 80 (ASTM, 1996) and surface area[14].

The functional groups present in the sample (AAAE) were determined using Buck Scientific M500 and Shimadzu FTIR 8400S spectrophotometers over a range of 4000 – 400cm^{-1}. Scanning electron microscopy (SEM) was used to picture the surface morphology of the activated carbon (AAAE).

2.3 Effect of adsorption system parameters

2.3.1 Effect of AAAE Particle size

The effect of AAAE particle sizes on the adsorption of EB was studied at different particle sizes from 75 µm - 850 µm. 1g each of the seven particle sizes under investigation were emptied into a number of 250ml-stoppered glass Erlenmeyers flasks containing 100ml of the adsorbate at 100mg/L initial concentration, 30 ± 2 ℃. The content of the flasks were stirred at 120rpm with thermostated water-bath shaker for 150mins. The adsorbent was then filtered off the solution. The concentration of the supernatant solution was measured using a UV-vis spectrophotometer. The % of dye ions adsorbed was calculated from (1):

$$\%\text{ads} = \frac{C_o - C_e}{C_o} \times 100 \qquad (1)$$

where C_o and C_e are initial and equilibrium concentrations of the aqueous solution respectively.

2.3.2 Effect of pH

With 1g adsorbent dosage and 75 µm particle size of each of the adsorbents in 100ml of 100mg/L of the adsorbate, EB, the effect of pH was studied. At a temperature of 30 ℃, the content of the flasks were stirred for 150 mins at a speed of 120rpm. pH adjusters (0.1M HCl and 0.1M NaOH) were used to alter the pH of the solutions prepared. The pH of solution was adjusted from 2 -10.

2.3.3 Effect of Adsorbent Dosage

Different adsorbent dosages (0.5, 0.8, 1, 2, 3, 4g) were used to study the effect of adsorbent dosage on adsorption process at room temperature, 75 µm, 150 mins, 120 rpm and initial dye concentration of 100mg/L.

2.4 Equilibrium studies

Langmuir, Freundlich and Dubinin–Radushkevich isotherm models were studied. At varying temperatures and equilibrium time of 120mins, q_e, amount of adsorbed dye per gram of the adsorbent (mg dye/g adsorbent) was obtained using equation 2:

$$q_e = \frac{(C_o - C_e)V}{m} \qquad (2)$$

Where C_o (mg/L) and C_e (mg/L) are initial and equilibrium dye concentrations, V(L) and m (g) represent volume of the solution and mass of dry adsorbent.

2.5 Kinetic study

The kinetics of the adsorption process was described by pseudo-first order, pseudo-second order and Elovich kinetic models at temperatures 30 ℃, 40 ℃ and 50 ℃. At defined time intervals, the concentration of dyes were measured. Equation (3) was used to calculate the amount of dye ions adsorbed (q_t) at time, t:

$$q_t = \frac{(C_o - C_e)V}{m} \quad (3)$$

2.6 Theory of adsorption isotherm and kinetics

2.6.1 Isotherm models

Adsorption isotherm describes how adsorbate interacts with adsorbents and this is critical in optimizing the use of adsorbents[14]. The Langmuir[12], Freundlich[15] and Dubinin–Radushkevich[16] isotherm models were studied. The linear forms of the investigated isotherm model are presented in the equations 4, 5 and 6 respectively:

$$\frac{1}{q_e} = \frac{1}{Q_o} + \frac{1}{Q_o K_L C_e} \quad (4)$$

$$\log q_e = \log K_f + \frac{1}{n}\log C_e \quad (5)$$

$$\ln q_e = \ln q_D - \beta\varepsilon^2 \quad (6)$$

Where q_e (mg/g) and C_e (mg/L) represent amount of dye adsorbed per gram of the adsorbent at equilibrium and the residual dye concentration respectively. Q_o(mg/g) is the maximum monolayer coverage capacity and K_L (L/mg) is the Langmuir constant related to energy of adsorption capacity. From linear plots of C_e/q_e versus C_e, the slope and intercepts gave the constants Q_o and K_L. K_f corresponds to Freundlich isotherm constant (mg/g), n is the adsorption intensity. For D-B isotherm, q_D, β , ε represent theoretical isotherm saturation capacity (mg/g), Dubinin–Radushkevich isotherm constant related to mean free energy of adsorption per mole of the adsorbate (mol^2/kJ^2) and Polanyi potential respectively.

2.6.2 Kinetic models

The study of kinetics for an adsorption process describes the rate of uptake of adsorbate on the adsorbent which in turn helps to predict the mechanism of sorption and the rate-controlling steps[17]. The experimental data were fitted into the following kinetic models: pseudo-first-order[9,18], pseudo second-order[19,20] and Elovich[21] kinetic model equations:

For Pseudo first-order kinetic model, a simple kinetics of adsorption is given by Lagergren rate equation:

$$\frac{dq_t}{dt} = K_1(q_e - q_t) \quad (7)$$

Where k_1 (min^{-1}) is the pseudo first-order adsorption kinetic parameter, q_t and q_e denote the amount adsorbed at time t (min) and at equilibrium both in mgg^{-1}. Applying conditions $q_t = 0$ at $t = 0$ and $q_t = q_t$ at $t = t$, we have:

$$\log(q_e - q_t) = \log q_e - \frac{K_1}{2.303}t \quad (8)$$

Mathematical expressions for the pseudo second-order kinetic model are presented thus:

$$\frac{dq_t}{dt} = K_2(q_e - q_t)^2 \quad (9a)$$

K_2 is the rate constant of pseudo second-order model. Equation (9b) is obtained by integrating equation (9a) and applying a boundary conditions of t=0 to t=t and qt=0 to qt=qt.

$$\frac{t}{q_t} = \frac{1}{K_2 q_e^2} + \frac{t}{q_e} \quad (9b)$$

The Elovich model is generally expressed as:

$$\frac{dq_t}{dt} = \alpha e^{-\beta q_t} \quad (10)$$

Integrating equation (10) and applying boundary conditions:

$$q_t = \frac{1}{\beta}\ln(\alpha\beta) + \frac{1}{\beta}\ln t \quad (11)$$

a and β define the initial adsorption rate (mg/gmin) and the extent of surface coverage and the activation energy for chemisorptions (gmg^{-1})[21].

2.7 Validity of Kinetic Model

The validity of the kinetic models under investigation was determined by the sum of squared errors (SSE,%)[22] and root mean square (RMS)[23]. SSE,% and RMS were calculated using the following equations:

$$\text{SSE},\% = \sqrt{\frac{\sum(q_{t,exp} - q_{t,cal})^2}{N}} \quad (12)$$

$$\text{RMS} = \sqrt{\frac{1}{N}\sum_{i=1}^{N}\left(\frac{q_{exp} - q_{cal}}{q_{exp}}\right)^2} \quad (13)$$

Where N is the number of data points. The lower the RMS and SSE values, the better will be the goodness of fit.

2.8 Thermodynamic studies

Equations (14)[9] and (15)[24] were employed to determine the thermodynamic parameters (Gibbs free energy change, ΔG^o, enthalpy change, ΔH^o and entropy change, ΔS^o).

$$\ln K = \frac{-\Delta H^\circ}{RT} + \frac{\Delta S^\circ}{R} \quad (14)$$

$$\Delta G^\circ = -RT\ln K \quad (15)$$

Where R (universal gas constant) = 8.314J/molK, *K* (L/mol) is the dependency of the equilibrium association constant ($K = K_L$, Langmuir constant) and T is the solution temperature.

3.0 Results and discussion

3.1 Characteristics of adsorbent

The physical properties of the adsorbent (AAAE) were examined to ascertain its effectiveness. The data in table 1 presents a result obtained from the evaluation of the physical properties of the adsorbent. From table 1, the low percentage ash content and percentage moisture content values recorded show that AAAE has low inorganic content and high fixed carbon, also extensive porosity in the carbon structure was introduced by the activation processes.

The value obtained for surface area depicts availability of large specific surface area for adsorption. Bulk density defines the amount of adsorbate the carbon can hold per unit volume. The value was measured to be 0.64gcm^{-2}

Table 1: Physical properties of AAAE

Sample	Surface area (m^2/g)	Ash content (%)	Moisture content (%)	pH	Bulk density (g/cm^{-2})
AAAE	187	4.84	3.1	6.8	0.64

Fourier transform infrared spectroscopy analysis

Figs 2 and 3 show plots of infra red transmittance against wave number for thermally activated almond endocarp (TAAE) and AAAE. The FTIR spectra presented were obtained to consider the possible outcome of the interaction between the functional groups of the biomass (TAAE) and chemical activating agent. Functional groups were assigned to distinct peaks of TAAE spectrum at 769.98 cm-1 (=C-H out of plane bending), 1028.43 (primary amine, CN stretch), 1134.98 (secondary amine, CN stretch), 1248.47 (in-plane C-H bending), 1558.70 (secondary amide N-H bending), 1671.65 (alkenyl C ≡ C stretch), 1829.70 (C=O stretch), 2357.62 (B-H stretch), 2833.22 (C-H stretch), 3113.17, 3722.23 (O-H stretch). For AAAE spectrum, notable peaks were registered at 463.9 (P-S Stretch), 633.64 (=C-H out of plane bending), 1033.88 (primary amine, CN stretch), 1139 (secondary amide N-H bending), 1492.95 (C=C stretch), 1492.95 (C=C stretch), 1640.51 (alkenyl C=C stretch), 2376.38 (B-H stretch), 3407.37, 3976.39 (O-H stretch)[25]. The results presented denote that some peaks were shifted or disappeared, and also new peaks were detected. These changes observed in the spectra represent interactive effects due to involvement of those functional groups during the chemical treatment of the adsorbent thus some modifications is likely to have occurred[13].

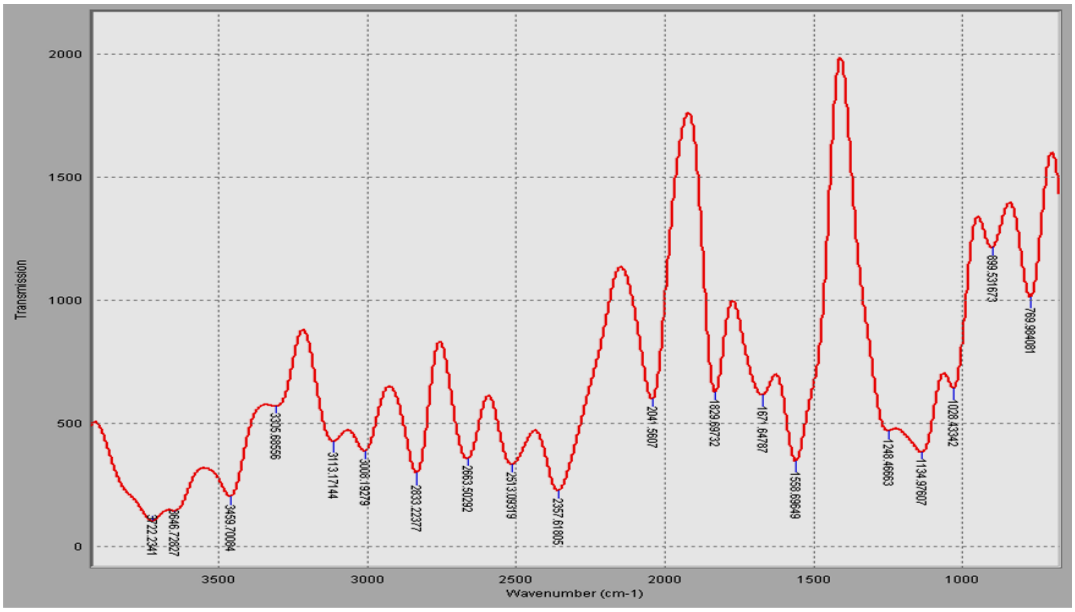

Fig 2: FTIR spectrum of thermally activated almond endocarp

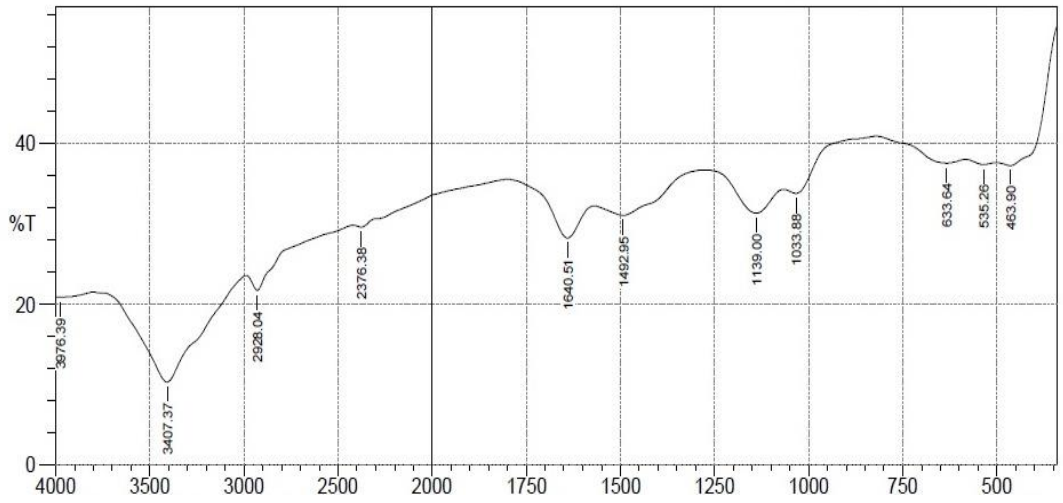

Fig 3: FTIR spectrum for acid activated almond endocarp

SEM Analysis

Scanning electron microscopy (SEM) is a key tool for characterizing the morphology of adsorbent surface. Fig 4 shows the morphology of the acid activated almond endocarp. The micrograph of AAAE presents a rough external surface with pores, cavities and cracks of different sizes. The characteristics found on the external structure of the adsorbent may be as a result of removal of some volatile matters during carbonization and also, evaporation of the impregnating mat

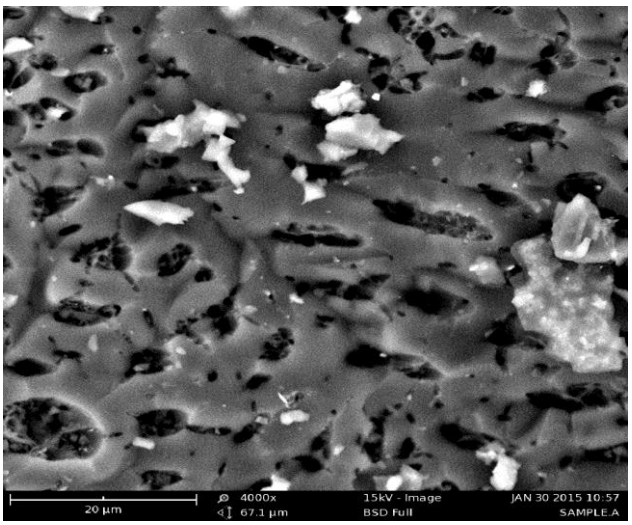

Fig 4: SEM micrograph for AAAE

3.2 Effect of Particle size

The effect of AAAE particle size on the adsorption of EB was evaluated. From fig 5, decrease in particle size had a positive effect on the percentage of dye adsorbed. Similar behaviour was reported by Arami *et al.* 2008. The trend followed by the graph may be explained by the fact that smaller sized particles have higher surface area, which in

turn favours adsorption and results in a shorter equilibration time[26]. For larger particles, the diffusion resistance to mass transfer is higher and most of the internal surface of the particle may not be utilized for adsorption thus decrease in the percentage of dyes adsorbed[27, 28].

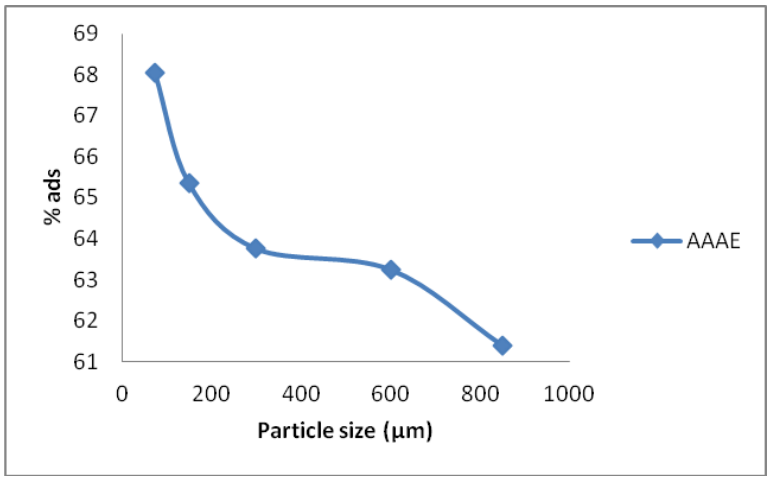

Fig 5: Effect of particle size on % EB adsorbed

3.3 Effect

Fig 6 show the influence of solution pH on AAAE. EB is anionic in nature. Activated carbon are species with amphoteric character, thus depend on the pH of the solution[9]. The pH of the solution may change the surface charge of the adsorbent, degree of ionization of the adsorbate molecule and extent of dissociation of functional groups on the active sites of the adsorbent[19]. Fig 6 shows that as pH moves from acidic to basic range, a decline in the percentage of EB dye adsorbed was observed for AAAE. Arami *et al.* 2008 had a similar result for adsorption of anionic dyes on egg shell membrane thus reported that at acidic range, a considerable high electrostatic attraction exists between the positively charged surface of the adsorbent, due to ionization of functional groups of adsorbent and negatively charged anionic dye molecules. The lower values recorded at basic pH range may be as a result that as pH value of the system increases, the surface charge of the adsorbents becomes more negatively charged hence electrostatic repulsion subsists between the dye molecules and surface charge of the activated carbon thus the poor adsorbance was recorded. A response of 95.75% was obtained for AAAE at pH 4.

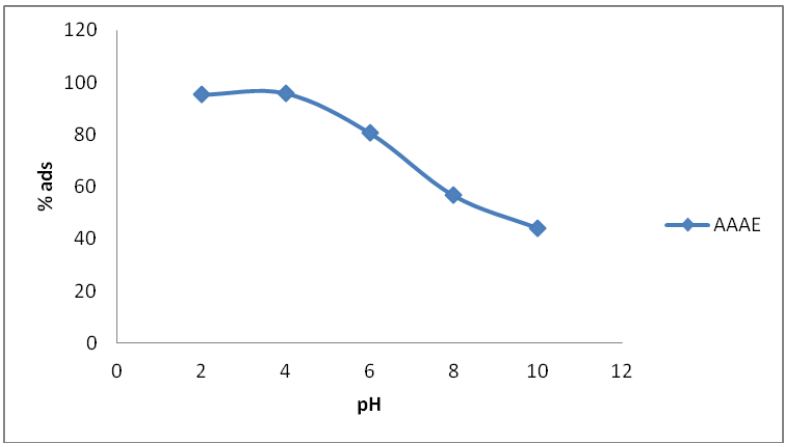

Fig 6: Effect of pH on % EB adsorbed

3.4 Effect of Adsorbent Dosage

The effect of varying dosage quantities on percentage of dye adsorbed was investigated to determine the least AAAE dosage for maximal response (percentage of dye adsorbed). Figure 7 indicated an initial distinct increment on the percentage of EB dye adsorbed for increased adsorbent dosage. The percentage of dye adsorbed rose from 71.51% to 98.9% for AAAE when the adsorbent dosage increases from 0.5g to 4g. The highest amount of dye adsorbed, 14.30mg/g for AAAE was recorded at 0.5g adsorbent dosage. Fig 7 shows that the amount of dye adsorbed per gram of adsorbent decreased with increase in adsorbent dosage. The percentage of dye adsorbed became almost constant when the dosage was increased above 1g thus 1g was chosen for further experiments. The increase in the percentages of dye adsorbed may be attributed to greater surface area and larger number of adsorption sites with an increase in adsorbent doses[29,30]. The decrease in unit adsorption with increasing dose of adsorbent is basically due to the adsorption sites remaining unsaturated during the adsorption process[31].

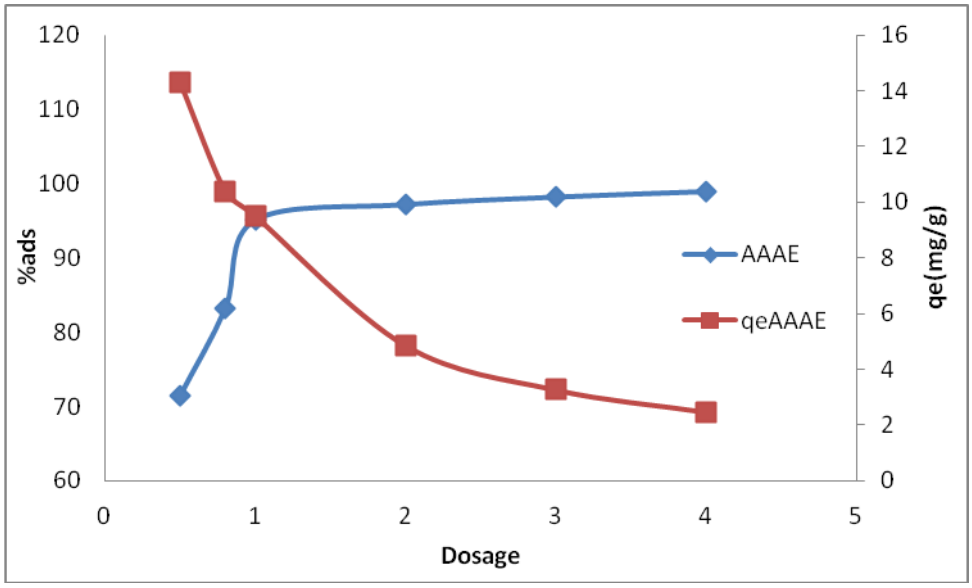

Fig 7: Effect of Dosage on % EB adsorbed

3.5 Effect of Concentration and Temperature

Fig 8 illustrates plot of amount of dye adsorbed per gram of the adsorbent against concentration at various temperatures. An increase in the amount of dye adsorbed was observed as concentration increased from 100 - 500mgL^{-1}. This is because the initial dyes concentration provides an important driving force to overcome all mass transfer resistances of the dye molecules between the aqueous and solid phases. Hence, a higher initial concentration of dye will enhance the adsorption process[32]. Temperature affects the rate of removal of dyes by altering the molecular interactions and the solubility of dyes[18]. Higher temperatures accelerate the rate of diffusion of the dye molecules from the surface to the internal pores of the adsorbent, also, temperature changes alter equilibrium between the adsorbent and the adsorbate[33]. While higher temperatures result in higher adsorption in endothermic processes, lower temperatures lead to higher adsorption in exothermic process.

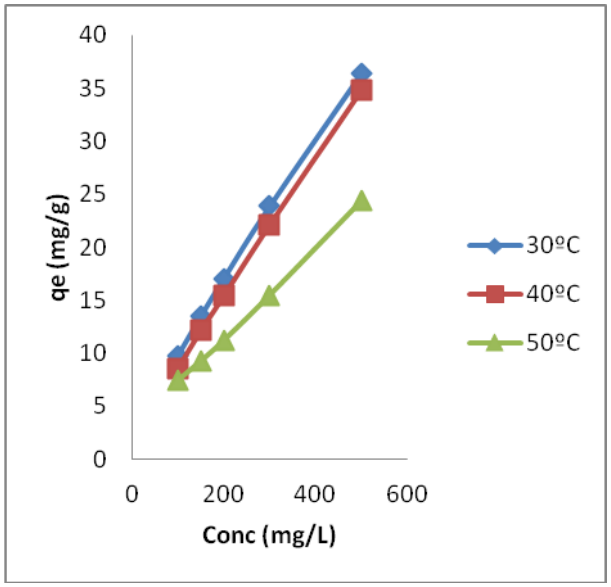

Fig 8: Effect of conc on amount of EB adsorbed

3.6 Effect of Time

The data for the uptake of EB against time was represented in fig 9. The result shows that the amount of dye, q_t (mg/g) increased with increase in time. At the initial stage, a rapid increase in the amount of dye adsorbed was observed. Beyond 60mins, the uptake of dye increased with a much slower rate after which a plateau was observed. The initial rapid increase of the amount of dye adsorbed may be due to the fact that at the beginning of the sorption process there were more vacant sites and hence the higher rate of uptake. The trend followed by the result obtained in fig 9 was also similar to what was reported by Hameed, 2009. The amount of dye adsorbed decreased with increase in temperature from 30 - 60 ℃ for AAAE. This behaviour may suggest some kind of exothermic nature of the adsorption process. According to Rao & Nair , 2006, the reason for the fall in the adsorption capacity at elevated temperatures may be that at higher temperatures a part of the dye leaves the solid phase and re-enters the liquid phase.

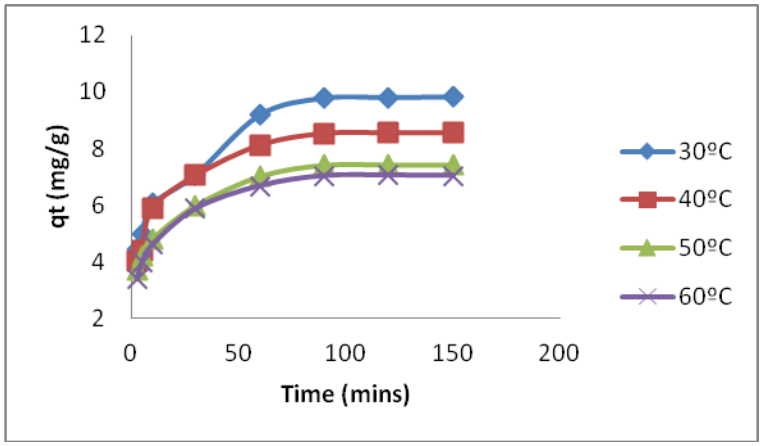

Fig 9: Effect of time on amount of EB adsorbed

3.7 Isotherm studies

Adsorption isotherm describes the relationship between the amount of adsorbate adsorbed and the adsorbent and the concentration of dissolved adsorbate in the liquid at equilibrium[24]. To study this relationship, the experimental data obtained were fitted over a wide range of concentration (100 – 500mg/L) and temperatures (303 – 323K) on Langmuir, Freundlich and Dubinin–Radushkevich isotherm models. Figs 10-12 represent plots of C_e/q_e vs C_e, log q_e vs log C_e and ln q_e vs ε^2. The Langmuir model assumes that the uptake of adsorbate molecules occurs on a homogeneous surface by monolayer adsorption without any interaction between adsorbed molecules[35]. Freundlich isotherm model describes the adsorption characteristics for the heterogeneous surface[15]. Dubinin-Radushkevich isotherm model is generally applied to express the adsorption mechanism with a Gaussian energy distribution onto a heterogeneous surface[16].

The suitability of the three isotherm models under investigation were based on coefficient of determination (R^2) values (table 2). The R^2 values of the Freundlich isotherm were closest to unity thus best described the experimental data obtained in the adsorption process. The favourablity of the adsorption of EB on AAAE was revealed using the separation factor (R_L). The Langmuir separation factor is mathematically expressed as:

$$R_L = \frac{1}{1+ K_L C_o} \qquad (16)$$

The value obtained for R_L indicates either unfavourable (R_L >1), linear (R_L = 1), favourable (0< R_L <1) or irreversible (R_L = 0) adsorption process[19]. Values presented for R_L in table 2 are between 0 and 1 implying a favourable uptake of EB on AAAE. Monolayer adsorption capacity between the range of 36.36 – 55.87mg/g were recorded.

The Freundlich heterogeneity factor, n, was calculated to be higher than 1 and lesser than 10 at all temperatures considered indicating that the adsorption of EB on AAAE was favourable. A smaller value of n indicates better adsorption and formation of relatively strong bond between adsorbate and adsorbent, respectively[36]. From table 2, the lowest value of heterogeneous factor (n) was recorded at temperature 313K. This is in agreement with the highest value recorded for Langmuir's adsorption capacity at the same temperature.

The poor R^2 values recorded for the Dubinin-Radushkevich isotherm model show that the model did not fit the experimental data thus did not describe the system.

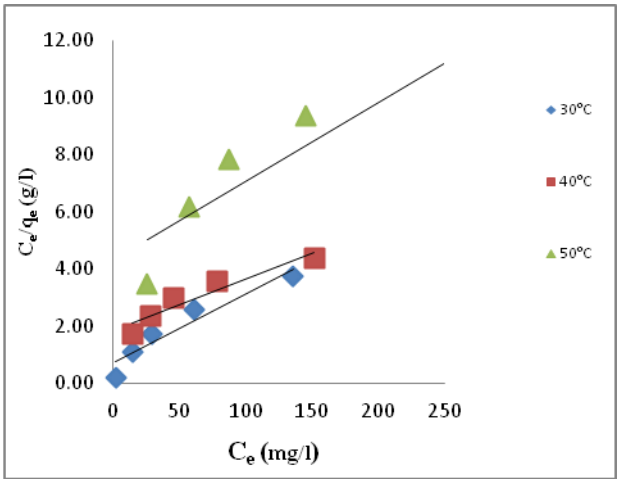

Fig 10: Langmuir Isotherm plot for EB on AAAE

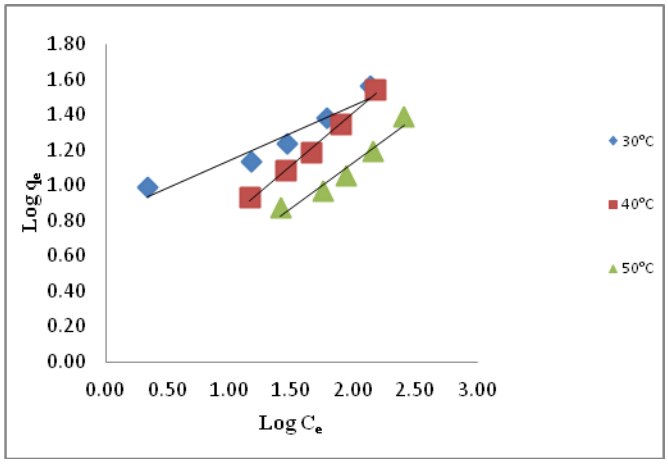

Fig 11: Freundlich Isotherm plot for EB on AAAE

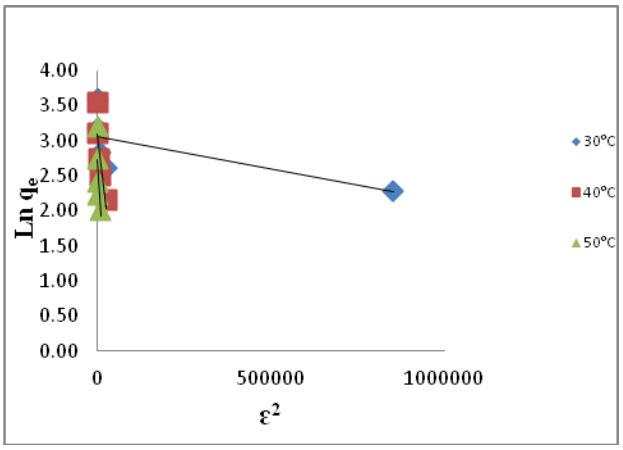

Fig 12: Dubinin–Radushkevich Isotherm plot for EB on AAAE

Table2: Calculated Isotherm parameters for the adsorption of EB on AAAE

	Langmuir				Freundlich			Dubinin-Radushkevich			
Temp	Q(mg/g)	K_L (L/mg)	R_L	R^2	n	K_f (L/g)	R^2	q_D (mg/g)	β (mol^2/J^2)	E (KJ/mol)	R^2
303	41.49	0.0347	0.2231	0.9174	3.2268	6.7671	0.9221	21.39	$9x10^{-7}$	0.745	0.4814
313	55.87	0.0096	0.5097	0.9058	1.6642	1.6282	0.9938	22.38	$4x10^{-5}$	0.112	0.6671
323	36.36	0.0064	0.9058	0.8158	1.9327	1.9327	0.9470	15.42	$1x10^{-4}$	0.071	0.5350

3.8 Kinetic studies

The kinetics of the adsorption of EB on AAAE was analyzed using the pseudo first-order, pseudo second-order and Elovich kinetic models. Figs 14 – 16 present non-linear plots of the models investigated. The conformity between the model predicted values and the experimental data was examined using root mean square (RMS) and sum of squared errors (SSE). The trend followed by the models under study in figs 14 – 16 show that the Elovich kinetic model best fitted the experimental data. Table 3 summarized kinetic and statistical parameters for the models studied. Increase in temperature increased the pseudo second order kinetic rate of adsorption (K_2) (see table 3). Figs 17 - 18 present histogram plots of the values of RMS and SSE recorded at various temperatures for the adsorption process. At all the temperatures considered, it was observed that the values of the RMS were ≤ 0.635, 0.135 and 0.043 for pseudo first-order, pseudo second-order and Elovich kinetic models respectively. From fig 18, plot of SSE values at various temperatures, the values recorded for pseudo second-order and Elovich kinetic models were ≤ 0.711 and 0.335 respectively. Higher values were recorded for pseudo first-order model (3.856 ≥ SSE ≥ 3.260). Based on these observations, Elovich kinetic model best described the kinetics of the system considering its lowest RMS and SSE values recorded compared to pseudo first-order and pseudo second-order models. Módenes *et al*, 2015 also reported that the Elovich kinetic model has provided better fits to the sorption kinetic data of RB5G dye at 20, 30 and 40 ℃ than the other two tested models (pseudo first-order and pseudo second-order), suggesting that the main mechanism is a chemisorptions process.

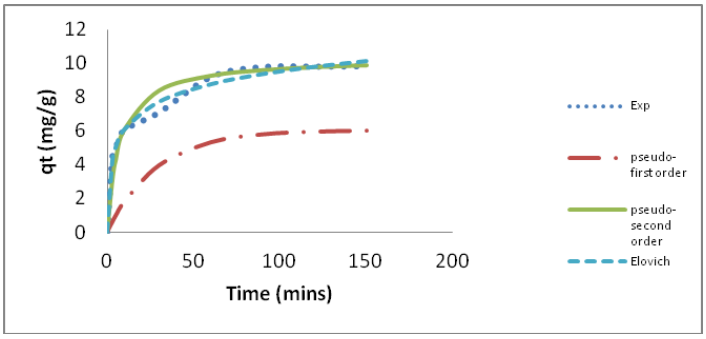

Fig 13: Kinetic Plot for the adsorption of EB on AAAE at 30 ℃

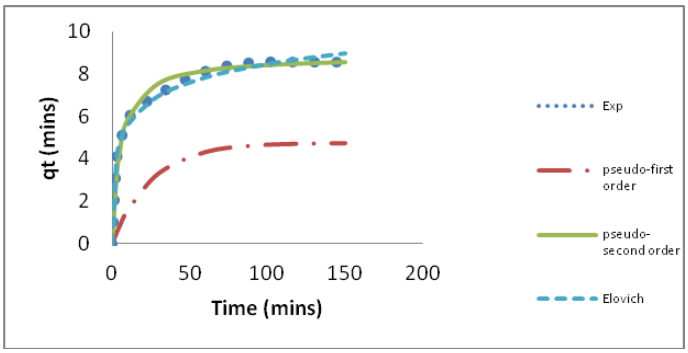

Fig 14: Kinetic Plot for the adsorption of EB on AAAE at 40 ℃

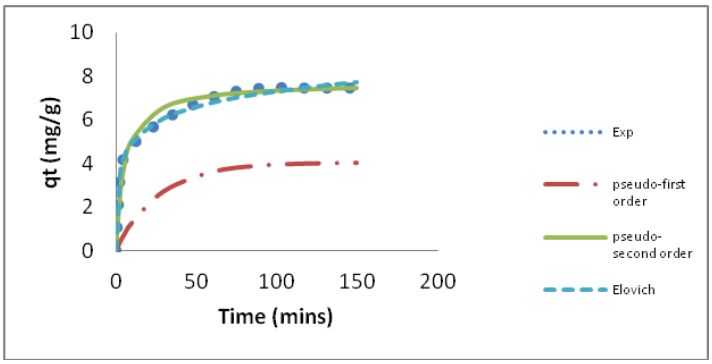

Fig 15: Kinetic Plot for the adsorption of EB on AAAE at 50 ℃

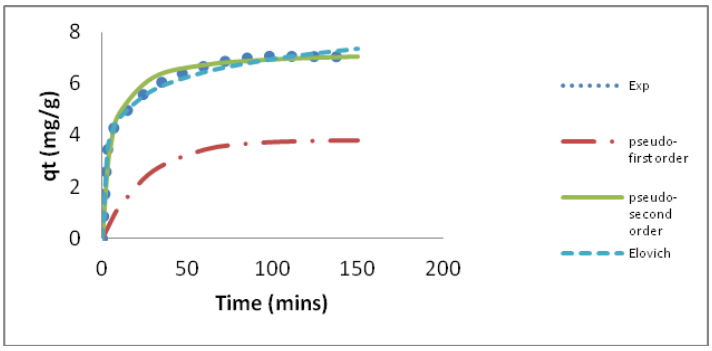

Fig 16: Kinetic Plot for the adsorption of EB on AAAE at 60 ℃

Table 3: Calculated kinetics parameters for the adsorption of EB on AAAE

Temp	Pseudo-first order					Pseudo-second order					Elovich				
	K_1 (min^{-1})	q_e (mg/g)	R^2	RMS	SSE	K_2 (g/mg min)	q_e (mg/g)	R^2	RMS	SSE	α (mg/g min)	B (g/mg)	R^2	RMS	SSE
30	0.0355	6.0364	0.9645	0.584	3.856	0.0138	10.3199	0.9972	0.135	0.711	8.6738	0.6680	0.9752	0.043	0.335
40	0.0401	4.7327	0.9876	0.618	3.828	0.0220	8.8731	0.9994	0.072	0.333	11.3699	0.8072	0.9784	0.041	0.258
50	0.0373	4.0181	0.9944	0.635	3.442	0.0245	7.7220	0.9990	0.104	0.431	12.5849	0.9758	0.9873	0.024	0.166
60	0.0391	3.8015	0.9974	0.632	3.260	0.0276	7.3046	0.9994	0.080	0.311	11.2397	1.0122	0.9862	0.025	0.164

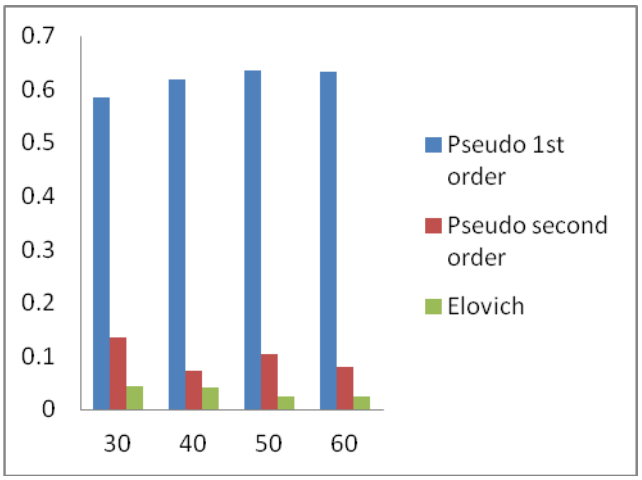

Fig 17: Comparative variation of RMS with temperature

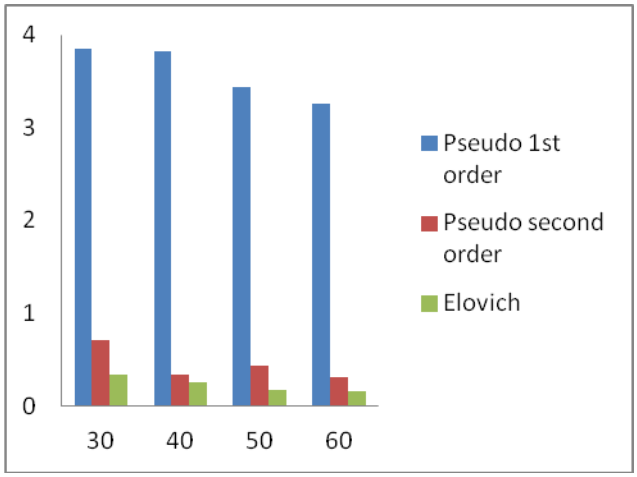

Fig 18: Comparative variation of SSE with temperature

3.9 Adsorption Thermodynamics

To evaluate the feasibility of the adsorption of EB on AAAE, thermodynamic parameters such as enthalpy change (ΔHº) and entropy change (ΔSº) were calculated from the slope and intercept of the plot of lnK against 1/T. Fig 19 represents plot of lnK against 1/T. The values of the Gibb's free energy, enthalpy and entropy changes are tabulated in Table 4. The negative ΔG^o indicates the spontaneous nature of the adsorption of EB dye on AAAE and also confirms the feasibility of the process. Negative enthalpy value obtained show that the process was exothermic in nature[22]. According to Oliveira *et al.* 2008, negative ΔSº value confirms the decreased randomness at the solid-solute interface during the adsorption process.

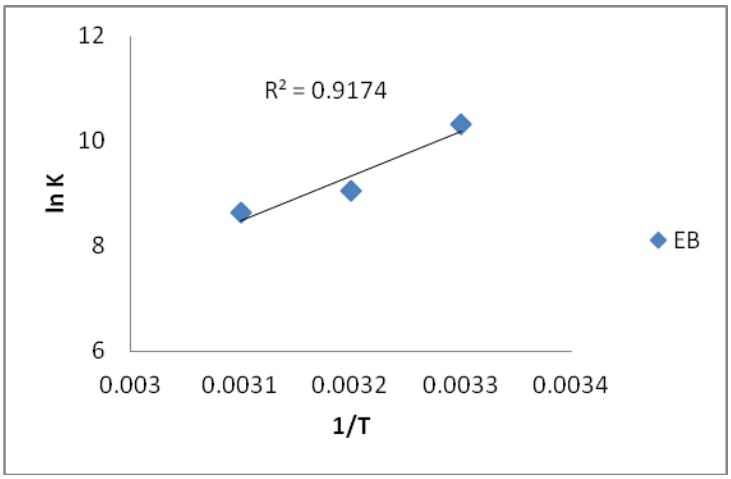

Fig 19: Thermodynamic plot for the adsorption of EB on AAAE

Table 4: Calculated thermodynamics parameters for the adsorption of EB on AAAE

Adsorbent	Thermodynamic parameters			
	T(K)	ΔG°(kJ/mol)	ΔH (kJ/mol)	ΔS (kJ/mol)
	303	-26.02		
AAAE	313	-23.53	-70.29	-0.147
	323	-23.19		

Conclusion

Activated carbon prepared from *Terminalia catappa* endocarp by thermal and chemical (acid treatment) activation was effective in the removal of EB dye from aqueous solution at various operating conditions. The characterization result presented the prepared activated carbon as a good adsorbent. Particle size, pH, adsorbent dosage, concentration, temperature and time had significant effect on the amount of EB dye adsorbed onto AAAE. Considering the coefficient of determination values obtained for the isotherm models investigated, the equilibrium adsorption data were best described by Freundlich isotherm model. Pseudo second-order and Elovich kinetic models presented lower RMS and SSE values compared to pseudo first-order therefore better fitted the experimental data. The negative values obtained for Gibbs free energy, enthalpy and entropy reveals that the process was feasible and spontaneous, exothermic and decreased randomness at the solid-solute interface.

References

1 Kousha, M., Daneshvar, E., Dopeikar, H, Taghavi, D. and Bhatnaga, A. (2012). Box-Behnken design optimization of acid black 1 dye biosorption by different brown macroalgae. Chemical Engineering Journal, 179, 158-168.

2 Uddin, M.T., Islam, M.A, Mahmud, S. and Rukanuzzaman, M. (2009). Adsorptive removal of methylene blue by tea waste. Journal of hazardous materials, 164, 53-60.

3 Kyzas, G.Z., Lazaridis, N.K., Mitropoulos, A.C.(2012). Removal of dyes from aqueous solutions with untreated coffee residues as initial low-cost adsorbents: Equilibrium, reuse and thermodynamic approach. Chemical engineering journal, 189-190, 148-159.

4 Ravikumar , K., Krishnan, Ramalingam, S. and Balu, K. (2007). Optimization of process variables by the application of response surface methodology for dye removal using a novel adsorbent. Dyes pigments, 72(1), 66-74.

5 Hameed, B.H. (2009). Removal of cationic dye from aqueous solution using jackfruit peel as non-conventional low-cost adsorbent. Journal of Hazardous Materials, 162, 344–350.

6 Stavropoulos, G.G. (2011). A fundamental approach in liquid phase adsorption kinetics. Fuel Processing Technology, 92, 2123-2126.

7 Oladoja, N.A., Aboluwoye, C.O., Oladimeji, Y.B, Ashogbon, A.O. and Otemuyiwa, I.O. (2007). Studies on castor seed shell as a sorbent in basic contaminated wastewater remediation. Deaslination, (227), 190-203.

8 Arami, M., Limaee, N,Y. and Mahmoodi, N.M. (2008). Evaluation of the adsorption kinetics and equilibrium for the potential removal of acid dyes using a biosorbent. Chemical Engineering Journal, 139, 2-10.

9 Al-Othman, A., Ali, R. and Naushad, M. (2012). Hexavalent chromium removal from aqueous medium by activated carbon prepared from peanut shell: Adsorption kinetics, equilibrium and thermodynamic studies. Chemical Engineering Journal, 184, 238-247.

10 Chowdhury, A.K., Sarkar, A.D. and Bandyopadhyay, A. (2009). Rice husk ash as low cost adsorbent for the removal of methylene blue and congo red in aqueous phases. Clean-journal.

11 Kushwaha, S., Sodaye, S and Padmaja, P. (2008). Equilibrium, kinetics and thermodynamic studies for adsorption of Hg (II) on palm shell powder. World Academy of Science, Engineering and Technology, 43, 600-606.

12 Oliveira, L.S., Franca, A.S., Alves, T.M. and Rocha, D.F. (2008). Evaluation of untreated coffee husks as potential biosorbents for treatment of dye contaminated waters. Journal of Hazardous materials. 155, 507-512.

13 Menkiti, M.C., Aneke, M.C., Ejikeme, P.M., Onukwuli, O.D. and Menkiti, N.U. (2014). Adsorptive treatment of brewery effluent using activated *Chrysophyllum albidium* seed shell carbon. Springer Plus, 3:213.

14 Nwabanne, J. T. and Igbokwe, P. K. (2012). Comparative Study of Lead (II) Removal from Aqueous Solution Using Different Adsorbents. International Journal of Engineering Research and Applications (IJERA), 2 (4), 1830-1838.

15 Hutson N. D. and Yang, R. T. (2000). Adsorption. J. Colloid Interf Sci., pp 189.

16 Gunay, A., Arslankaya, E. and Tosun, I. (2007). Lead removal from aqueous solution by natural and pretreated clinoptilolite: adsorption equilibrium and kinetics. J.Hazard. Mater. 146, 362–371.

17 Saha, P., Chowdhury, S., Gupta, S., Kumar, I. and Kumar, I. (2010). Assessment on the removal of malachite green using tamarind fruit shell as biosorbent. Clean-Journal, 38 (5-6), 437-445.

18 Verma, V.K. and Mishra A.K. (2010). Kinetic and isotherm modelling of adsorption of dyes onto rice husk carbon. Global Nest Journal, 12(2), 190-196.

19 Ramachandran, P., Vairamuthu, R. and Ponnusamy, S. (2011) Adsorption isotherms, kinetics, thermodynamics and desorption studies of reactive orange 16 on activated carbon derived from *Ananas cosmosus* (L.) carbon. ARPN Journal of Engineering and Applied Sciences. 6(11), 15-26.

20 Sun, Q. and Yang, L. (2003). The adsorption of basic dyes from aqueous solution on modified peat-resin particle. Water research, 37, 1535-1544.

21 Namasivayam, C. and Kavitha, D. (2002). Removal of congo red from water by adsorption onto activated carbon prepared from coir pith, an agricultural solid waste. Dyes and Pigments. 54, 47-58.

22 Tan, I.A.W., Ahmed, A.L. and Hameed, B.H. (2008). Adsorption of basic dye on high-surface-area activated carbon prepared from coconut husk: Equilibrium, kinetics and thermodynamic studies. Journal of Hazardous Materials, 154, 337-346.

23 Kitanovic, S., Milenovic, D. and Veeljkovic, V.B. (2008). Empirical kinetic models for resinoid extraction from aerial parts of St john's Wort (*Hypericum perforatum).* J.Biochem. Eng. 41, 1-11.

24 Rameshraja, D., Srivastava, V.C., Kushwaha, J.P. and Mall, I.D. (2012). Quinoline adsorption onto granular activated carbon and bagasse fly ash. Chemical Engineering Journal, (181-182), 343-351.

25 Coates, J. (2000). Interpretation of Infrared spectra, a practical approach. In Encyclopedia of analytical chemistry (pp 10815-10837). Chichester: John Wiley and sons ltd.

26 Osasona, I., Ajayi, O. O. and Adebayo, A. O. (2014). Equilibrium, Kinetics, and Thermodynamics of the Removal of Nickel(II) from Aqueous Solution Using Cow Hooves. Advances in Physical Chemistry, http://dx.doi.org/10.1155/2014/863173.

27 Anndurai, A., Babu, S.R., Mahesh, K.P.O. and Murugesan, T. (2000). Adsorption and biodegeneration of phenol by chitosan-immobilized pseudomonas putida (NICM 2174). Bioprocess engineering, 2, 493-501.

28 Agarry, S.E., Aremu, M.O. and Ajani, A.O. (2013). Modelling the simultaneous adsorption and biodegeneration of aromatic hydrocarbons onto non-carbonized biological adsorbent in batch system. Chemical and Process engineering research, 12, 9-18.

29 Mohd Salleh, M.A., D.K. Mahmoud, W.A. Wan Abdul Karim, A. Idris, Cationic and anionic dye adsorption by agrigultural solid wastes: a comprehensive review, Desalination 280 (2011) 1-13.

30 Ofomaja, A.E. (2008). Sorptive removal if methylene blue from aqueous solution using palm kernel fibre: effect of fibre dose, Biochem. Eng.J. 40, 8-18.

31 Somasekhara, M.C., Sivaramakrishna, L. and Varada A. (2012). The use of an agricultural waste material, Jujuba seeds for the removal if anionic dye (Congo red) from aqueous medium. Journal of Hazardous Materials, 203-204, 118-127.

32 Bayramoglu, G., Altintas, B. and Arica, M. (2009). Adsorption kinetics and thermodynamic parameters of cationic dyes from aqueous solutions by using a new strong cation-exchange resin. Chemical Engineering Journal. 152, 339-346.

33 Schimmel, D., Fagnani, K.C., Santos, J.B., Barros, M.A. and Silva, E.A. (2010). Adsorption of turquoise blue QG reactive bye commercial activated carbon in batch reactor: kinetic and equilibrium studies. Brazilian Journal of Chemical Engineering, 27 (2), 289-298.

34 Rao, J., Aravindhan, R. and Nair, B. (2006). Removal of basic yellow dye from aqueous solution by sorption on green alga *Caulerpa scalpelliformis.* Journal of Hazardous Materials, doi:10.1016/j.

35 Deng , H., Yang, L., Tao, G. and Dai, J. (2009). Preparation and characterization of activated carbon from cotton stalk by microwave assisted chemical activation-application in methylene blue adsorption from aqueous solution. Journal of Hazardous Materials, 166, 1514-1521.

36 Dada, A.O., Olalekan, A.P., Olatunya, A.M. and Dada, O. (2012). Langmuir, Freundlich, Temkin and Dubinin–Radushkevich isotherms studies of equilibrium sorption of Zn^{2+} unto phosphoric Acid modified rice husk. Journal of Applied Chemistry, 3(1), 38-45.

37 Módenes, A.N., Espinoza-Quiñones, F.R., Geraldi, A.Q., Manenti, D. R., Trigueros, E.G., Oliveira, A.P., Borba C.E. and Kroumov, A. D. (2015) Assessment of the banana pseudostem as a low-cost biosorbent for the removal of reactive blue 5G dye. Environmental Technology, 36:22